Quantitative thermoreflectance imaging : calibration method and validation on a dedicated integrated circuit

G. Tessier, S. Pavageau, C. Filloy, B. Charlot, G. Jerosolimski, D. Fournier, B. Cretin, S. Dilhaire, S. Gomes, N. Trannoy, et al.

Belgirate, Italy, 28-30 September 2005

QUANTITATIVE THERMOREFLECTANCE IMAGING: CALIBRATION METHOD AND VALIDATION ON A DEDICATED INTEGRATED CIRCUIT

G. Tessier [1], S. Pavageau[1], C. Filloy[1], B. Charlot[2], G. Jerosolimski[1] and D. Fournier[1], B. Cretin[3], S. Dilhaire[3], S. Gomes[3], N. Trannoy[3], P. Vairac[3] and S. Volz[3]

[1] UPR A0005 CNRS, ESPCI, Laboratoire d'optique, 10 rue Vauquelin, 75005 Paris, France
[2] TIMA, 46 Avenue Félix VIALLET, 38031 Grenoble, France.
[3] Groupement de Recherche Micro et Nanothermique, GDR CNRS 2503, Ecole Centrale Paris, Grande Voie des Vignes, 92295 Châtenay Malabry, France

ABSTRACT

We have developed a CCD-based thermoreflectance microscope which can deliver thermal images of working integrated circuits. However, in any thermoreflectance experiment, the coefficient linking reflectance variations to temperature is different for each material. Calibrations are therefore necessary in order to obtain quantitative temperature imaging on the complex surface of an integrated circuit including several materials such as aluminium and polysilicon. We propose here a system using a Peltier element to control the temperature of the whole package in order to obtain calibration coefficients simultaneously on all the materials visible on the surface of the circuit. Under high magnifications, vertical and lateral movements associated to thermal expansion are corrected using respectively a piezo electric displacement and a software image shift. This calibration method has been validated by comparison with the temperatures measured with separately calibrated thermocouples and diodes placed close to the integrated resistors.

1. INTRODUCTION

Thermoreflectance microscopy can deliver thermal images with high spatial resolutions by measuring the variations of the reflection coefficient with temperature. Since it can work at visible or even UV wavelengths, it is a unique tool to measure the temperature mapping of integrated circuits with submicronic features. Thermoreflectance uses the relationship linking the optical reflectivity R(T) and the temperature T of a given material, which is linear in a first approximation:

$$R(T) \approx R(T_0) + \frac{\partial R}{\partial T}(T - T_0) . \quad (1)$$

Given $R(T_0)$ and T_0, T can therefore be derived from the optical measurement of R(T). However, since $\partial R/\partial T$ is generally of the order of 10^{-3} to 10^{-5} K^{-1}, heat modulation and lock-in detection techniques are used, whether for single probes or for spatially multiplexed measurements [1]. In the latter approach, which is adopted here, the temperature-induced reflectivity variations are detected using a CCD camera synchronized with the heating phenomenon [1, 2] , as described in figure 2. The temperature field cannot be easily measured in continuous regime with these modulated techniques. However, a good approximation is obtained by modulating the bias at a frequency F for which the thermal diffusion length μ is larger than the investigated area.

2. SAMPLE DESCRIPTION

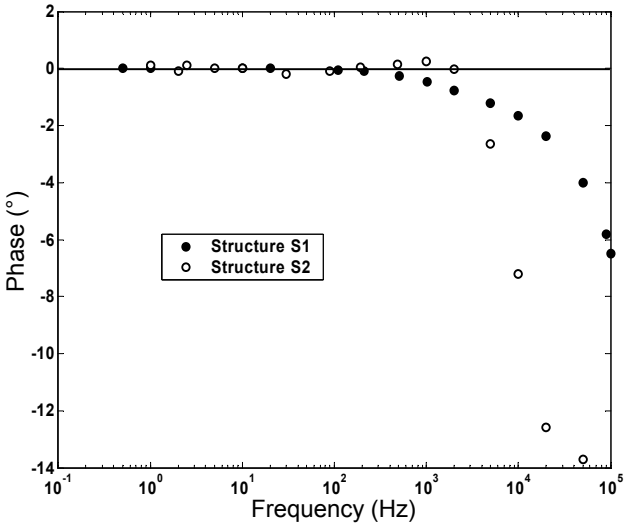

Figure 1: Relative phase of the voltage applied to the resistor and of the temperature modulations. The temperature is measured with a diode in the vicinity of the resistor in the case of S1 and with a thermocouple stack deposited on the resistor itself in S2. The shape of the devices and their thermal constants explain the different cutoff frequencies: 200 Hz for S1 and 2 kHz for S2.

 ISBN 2-916187-01-4

In order to check the accuracy of thermoreflectance measurements, several integrated structures dedicated to thermoreflectance calibration have been designed and implemented on a standard 0.35 µm CMOS technology. They include resistors of different shapes and sizes, coupled to either thermocouple stacks (polysilicon/aluminium) or diodes used as temperature sensors. These sensors can be calibrated by a separate technique, and therefore be used as an external temperature reference.

The first structure (S1, see inset in figure 5, left) studied here is a loop-shaped polysilicon resistor (R=109 Ω, 30 x 44 µm) surrounding a diode. The temperature dependence of the voltage drop at the diode has been measured by applying a constant temperature comprised ranging between 25 and 200 °C in an oven. In this range, which is approximately the temperature range reached by the resistor without damage, the behaviour of the diode is very linear, and we measured a slope of $-1.42\ 10^{-3}$ V.K^{-1}.

The other structure (S2, see inset in figure 5, right) is a broad 100 x 100 µm resistor (17.8 Ω) on which a series of ten polysilicon/aluminium junctions is deposited. Each structure forms an independent heater/sensor couple. Before we perform thermoreflectance measurements at low frequency, we must check the accuracy of the comparison between DC and low frequency AC temperature measurements. Using a lock-in amplifier, we have measured the relative phase of a sine voltage (V_{pp}= 4 V) applied to each resistor and the temperature measured with either the diode or the thermocouple. As can be seen in figure 1, the electric excitation and the temperature are perfectly in phase at low frequencies. A phase difference appears in S1 above 100 Hz, and above 2 kHz in S2. This is qualitatively explained by the fact that the thermocouple is just on top of the resistor in structure S2. A large phase difference is obtained when the thermal diffusion length becomes of the order of the thickness of the insulating layer separating them. In structure S1, this happens at lower frequencies since the diode is a few microns away from the resistor.

Both these measurements confirm that the temperature obtained at a low heating frequency (a few tens of Hertz) is perfectly comparable to the temperature obtained in static regime, and that there is little distortion of the temperature modulation with respect to the electrical excitation.

3. CALIBRATION SET-UP

To obtain a quantitative temperature, the coefficient $\frac{1}{R(T_0)}\frac{\partial R}{\partial T}$ has to be measured precisely. This requires an external temperature measurement. One method is to use a micro-thermocouple to measure a local temperature[1] . Here, we chose to use a Peltier element to control the temperature of the whole device precisely with a feedback loop. A similar technique has already been applied to single beam thermoreflectance[3] , but several important adaptations are required in the case of CCD-based thermoreflectance, as shown here. Since we are not using a coherent illumination, the interference effects which have been observed by authors using laser probes[3] do not occur in our case, even at high magnification.

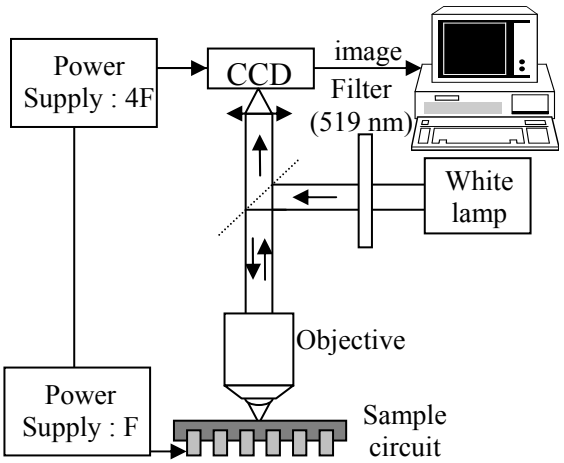

Figure 2 : CCD-based thermoreflectance set-up for integrated circuits thermal imaging.

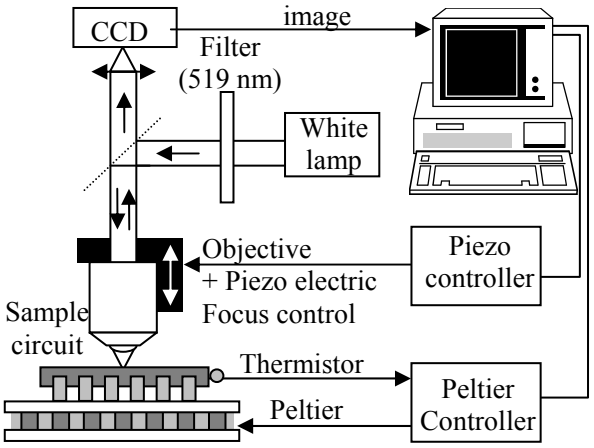

Figure 3 : Configuration for the measurement of the calibration coefficient dR/dT. The temperature of the disconnected electronic device is controlled. For each temperature, image processing determines the lateral displacement and the best focusing.

Due to the long time constant of packaged devices, applying an external temperature modulation would require extremely low frequencies (a few mHz) for which a lock-in detection becomes subject to drifts. We have acquired CCD images for various temperatures T and

calculated the average of the image level I(T) in homogeneous regions of interest. Since $\frac{I(T)}{I(T_0)} = \frac{R(T)}{R(T_0)} \approx 1 + \frac{1}{R(T_0)}\frac{\partial R}{\partial T}(T - T_0)$, a linear fit to the values of $\frac{I(T)}{I(T_0)}$, gives a slope $\frac{1}{R(T_0)}\frac{\partial R}{\partial T}$. The signal-to-noise ratio is relatively poor since no lock-in technique can be used here, but this can eventually be overcome by taking many measurements of I(T).

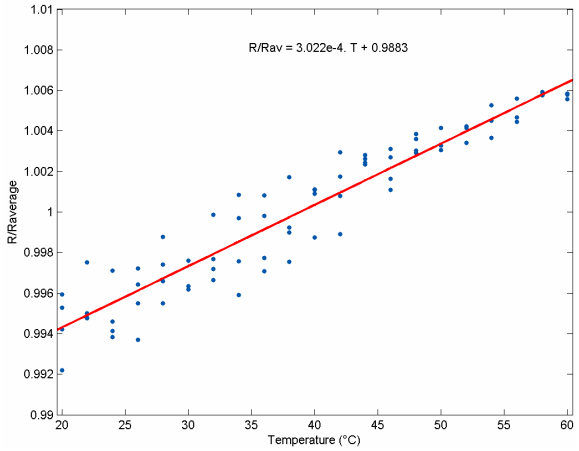

Figure 4: Calibration curve obtained on passivated polysilicon illuminated at λ=591 nm.

The main experimental problems are linked to thermal expansion of the device. An important vertical movement of the sample is observed, which causes defocusing and therefore information loss. The position of the optimal focus has to be determined in order to mechanically correct the position of the objective. This is relatively straightforward in an imaging setup: the sharpness of the image is obtained by calculating the average value of a 2D gradient (spatial derivative) over the image. By plotting the value of this parameter for several positions of the objective, a maximum can be extracted, corresponding to the best focus. Under high magnifications, a lateral displacement caused by inhomogeneous expansion is also observed. This movement causes no information loss, but has to be corrected in order to be able to measure the reflectivity of a chosen region of the sample. We obtain the lateral displacement by calculating the translation that optimizes the correlation of the current image with a reference image.

The procedure to obtain a calibration has been fully automated using the setup described in figure 3, and follows the sequence : 1) Fix a temperature T and wait for the thermalisation of the integrated circuit package. 2) Find the best focus. 3) Correct lateral translations of the image. 4) Measure the reflectivity R(T) in one or more regions of the image. Repeating this procedure gives as many points as necessary in order to obtain a good reliability of the linear fit. An example of this measurement on the polysilicon resistor S1 is shown in figure 4, and gives $\frac{1}{R(T_0)}\frac{\partial R}{\partial T} = 3.10^{-4}$ K^{-1} at an illumination wavelength centered at λ=591 nm (15 nm FWHM). This value is strongly material and wavelength dependent, and is strongly affected by interference in the transparent passivation layer [2] .

4. SIGNAL PROCESSING

Once the calibration is achieved, the set up described in figure 2 can be used to measure local reflectivity variations and deduce a temperature map. However, the sampling which is obtained with a CCD camera is not ideal. CCD cameras cannot deliver an instantaneous value of the light flux, but merely integrate photons over a given time. For this reason, deriving an exact value for the amplitude of the reflectivity variations is not as straightforward as with a conventional single detector lock-in technique. The usual method is to acquire 4 images (I_1 to I_4) per period of the modulated phenomenon to be studied, each integrated over ¼ of the period. The amplitude and phase of this modulation are then qualitatively obtained using the modulus and phase of the complex number [4, 5] : $A = I_1 - I_3 + j(I_2 - I_4)$. (2)
This is usually sufficient when doing qualitative imaging. However, in the quantitative approach taken here, a calculation of the spectrum obtained with this integrated sampling shows that it is necessary to take corrective coefficients into consideration, depending on the type of modulation considered. In our case, the temperature is modulated with an amplitude ΔT, which creates a modulation of the reflectivity with an amplitude ΔR. If R is sine-modulated, we obtain :

$$\left|\frac{\Delta R}{R_0}\right| = \frac{\pi}{\sqrt{2}}\frac{|A|}{I_0}, \quad (3)$$

where $I_0=(I_1+I_2+I_3+I_4)/4$ is the average of the four images. If the phenomenon to be measured is a square modulation, odd harmonics appear and the calculation, although slightly longer, yields a similar result:

$$\left|\frac{\Delta R}{R_0}\right| = \sqrt{2}\frac{|A|}{I_0}. \quad (4)$$

5. EXPERIMENTAL RESULTS

We have used the setup described in figure 2 to obtain images of the reflectivity variations on the surface of resistors S1 and S2 under bias. The excitation was a low frequency F=7.5 Hz square modulation from 0 to 4V. Since the cutoff frequency of our system is much higher

than 7.5 Hz, as seen in section 2, we can assume the temperature modulation, and therefore the reflection coefficient modulation, to be square. The sampling was done using a CCD camera triggered at 4F=30 Hz, with an exposure time of 31 ms, almost equal to 1/4F (the electronic transfer of the image takes about 1.8 ms). The F and 4F modulations are generated by synchronized generators using the same clock signal. In these conditions, applying eq.(4) and using the calibration coefficient obtained in section 3, we obtain the temperature map shown in figure 5.

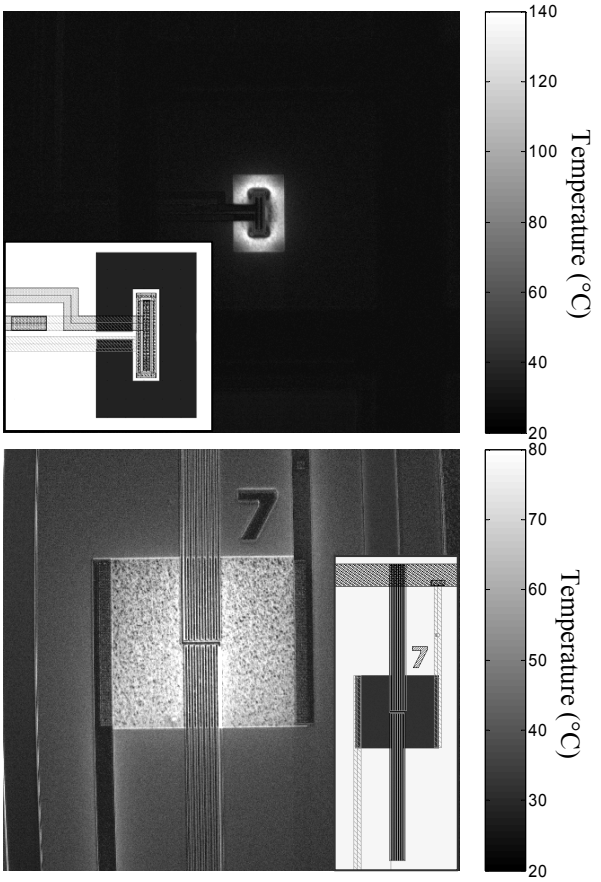

Figure 5 : Thermal images (250 x 250 µm) obtained on the integrated polysilicon resistors S1 (left) and S2 (right), under a square modulation with F=7.5 Hz and V_{pp}=4 V. Note that the color bar gives the absolute temperature in the polysilicon resistor only. The insets show the layouts of each structure, with the diode clearly visible at the center of S1, and the ten thermocouple junctions at the center of S2.

In the same conditions, we have measured the voltage drop in the diode of structure S1: Vd = 0.673 V. With a slope of -1.42 10^{-3} $V.K^{-1}$ (see section 2) and Vd = 0.822 V at room temperature (26 °C), we obtain a temperature of 131 °C. This is in good agreement with the temperatures measured on the resistor which are, as can be seen in figure 5, in the 120-140 °C range. The temperatures measured on S2 are around 70°C in the same conditions, since the power density is lower. The calibration of the thermocouple stack can be obtained using this temperature. This calibration coefficient will be compared to the coefficients obtained with a specially designed structure implemented on the same chip.

6. CONCLUSION

We have presented a fully automated system dedicated to the calibration of CCD-based thermoreflectance experiments, which can measure $\frac{1}{R(T_0)}\frac{\partial R}{\partial T}$ for any illumination wavelength in the visible range. Using this coefficient, CCD thermoreflectance can give a quantitative temperature image on an integrated resistor, which is in good agreement with the temperature obtained by a diode measurement. However, since the temperature is not homogeneous on the resistor, it is difficult to check the accuracy of this comparison with a precision better than a few degrees. The second structure, S2, which shows a more homogeneous temperature distribution would be more adapted to this purpose once the thermocouple stacks are calibrated.

The authors acknowledge funding and support from the “Groupement De Recherche micro et nanothermique” of the Centre National de la Recherche Scientifique (GDR 2503 CNRS).

7. REFERENCES

[1] G. Tessier, S. Hole and D. Fournier, "Quantitative thermal imaging by synchronous thermoreflectance with optimized illumination wavelengths", *Applied Physics Letters*, **78**, 2267-2269, 2001
[2] G. Tessier, G. Jerosolimski, S. Hole, D. Fournier and C. Filloy, "Measuring and predicting the thermoreflectance sensitivity as a function of wavelength on encapsulated materials", *Review of Scientific Instruments*, **74**, 495-499, 2003
[3] S. Dilhaire, S. Grauby and W. Claeys, "Calibration procedure for temperature measurements by thermoreflectance under high magnification conditions", *Applied Physics Letters*, **84**, 822-824, 2004
[4] P. Gleyzes, F. Guernet and A. C. Boccara, "Picometric profilometry .2. Multi detector approach and multiplexed lock-in detection", *Journal of Optics-Nouvelle Revue D Optique*, **26**, 251-265, 1995
[5] S. Grauby, B. C. Forget, S. Hole and D. Fournier, "High resolution photothermal imaging of high frequency phenomena using a visible charge coupled device camera associated with a multichannel lock-in scheme", *Review of Scientific Instruments*, **70**, 3603-3608, 1999